The Optimal Paper Moebius Band

Richard Evan Schwartz *

May 19, 2024

Abstract

We prove that a smooth embedded paper Moebius band must have aspect ratio greater than $\sqrt{3}$. We also prove that any sequence of smooth embedded paper Moebius bands whose aspect ratio converges to $\sqrt{3}$ must converge, up to isometry, to the triangular Moebius band. These results answer the mimimum aspect ratio question discussed by W. Wunderlich in 1962 and prove the more specific conjecture of B. Halpern and C. Weaver from 1977.

1 Introduction

1.1 The Triangular Moebius Band

To make a paper Moebius band you give a $1 \times \lambda$ strip of paper an odd number of twists and then join the ends together. For long strips this is easy and for short strips it is difficult or impossible. Let me first discuss a beautiful example, known as the *triangular Moebius band*. Figure 1a shows the triangular Moebius band. It is based on a $1 \times \sqrt{3}$ strip.

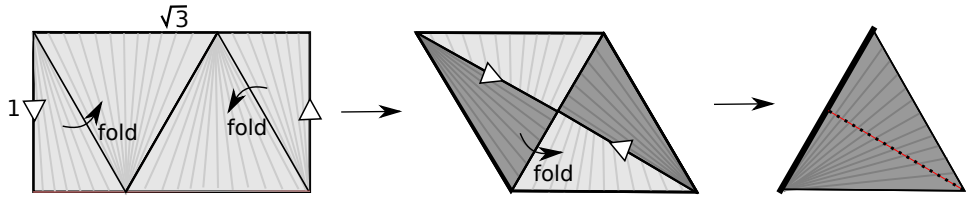

Figure 1a: The triangular Moebius band

*Supported by N.S.F. Grant DMS-2102802, a Simons Sabbatical Fellowship, and a Mercator Fellowship.

The strip in Figure 1a is lightly shaded on one side and darkly shaded on the other. First fold the flaps in to make a rhombus, then fold the rhombus in half like a wallet. This folding brings the two ends together with a twist. The dotted segment indicates where the ends are joined. The bold segment indicates the "wallet fold". The dotted and bold segments together make a pattern like a T. The pinstriping exhibits the strip as a union of line segments, disjoint except at the endpoints, which stay straight during the folding.

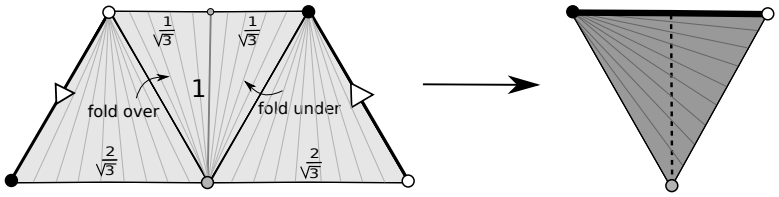

Figure 1b: The triangular Moebius band: another view

Figure 1b shows another view. Here we start with a symmetric trapezoid rather than a rectangle, but we get the same object when we fold and join the sides together. The bold edge indicates where the sides are joined. The dotted and bold segments again make a "T-pattern".

The triangular Moebius band goes back at least to the 1930 paper [**Sa**] of M. Sadowski. Technically, it does not quite fit the definition of a (smooth, embedded) paper Moebius band that we give below, but it is the limit of such. The triangular Moebius band is probably best considered as a *folded ribbon knot*. See [**DL**] for this point of view.

1.2 The Minimum Aspect Ratio Question

The triangular Moebius band looks like an extremely efficient construction. Can we do better in terms of making λ smaller? To answer this question in a meaninful way, we first need a formal definition.

Definition: A *smooth paper Moebius band of aspect ratio* λ is an infinitely differentiable isometric mapping $I : M_\lambda \to \boldsymbol{R}^3$, where M_λ is the flat Mobius band obtained by identifying the length-1 sides of a $1 \times \lambda$ rectangle. That is:

$$M_\lambda = ([0,\lambda] \times [0,1])/\sim, \qquad (0,y) \sim (\lambda, 1-y). \tag{1}$$

An *isometric mapping* is a map which preserves arc-lengths. The map is an *embedding* if it is injective, and an *immersion* in general. Let $\Omega = I(M_\lambda)$. We often write $I : M_\lambda \to \Omega$. We call Ω *embedded* when I is an embedding.

The early papers of M. Sadowsky [**Sa**] and W. Wunderlich [**W**] treat both the existence and differential geometry of smooth paper Moebius bands. (See [**HF**] and [**T**] respectively for modern English translations.) The paper [**CF**] gives a modern differential geometric framework for developable surfaces like Ω. The papers [**CK**], [**KU**], [**RR**] and [**Sab**] are all studies of the differential geometry of paper Moebius bands. I learned about paper Moebius bands from the great expository article [**FT**, Chapter 14] by Dmitry Fuchs and Sergei Tabachnikov.

Why bother with smooth maps? Well, if you just look at ways of folding paper up to make a Moebius band you can get weird examples which render the main question meaningless. For instance, you could fold any rectangle (e.g. a square) like an accordion into a thin strip, twist, then tape. The smooth formalism efficiently rules out the Moebius-accordion and other kinds of origami monsters. They are not limits of smooth paper Moebius bands. In contrast, the triangular Moebius band is the limit of smooth (embedded) paper Moebius bands. See [**Sa**], [**HW**], and [**FT**]. Basically you just use a slightly longer piece of paper and round out the sharp folds.

I imagine that the minimum aspect ratio question has been around for as long as people have been making paper Moebius bands, but in any case W. Wunderlich discusses this in the introduction of his 1962 paper [**W**]. In their 1977 paper [**HW**], Ben Halpern and Charles Weaver study the minimum aspect ratio question in detail. They prove two things.

- For smooth immersed paper Moebius bands one has $\lambda > \pi/2$. Moreover, for any $\epsilon > 0$ one can find an immersed example with $\lambda = \pi/2 + \epsilon$.
- There exists some $\epsilon_0 > 0$ such that $\lambda > \pi/2 + \epsilon_0$ for a smooth embedded paper Moebius band. This ϵ_0 is not an explicit constant.

On the last line of [**HW**], Halpern and Weaver conjecture that $\lambda > \sqrt{3}$ for a smooth embedded paper Moebius band. In this paper I will resolve the Halpern-Weaver conjecture.

Theorem 1.1 (Main) *A smooth embedded paper Moebius band has aspect ratio greater than* $\sqrt{3}$.

Theorem 1.2 (Triangular Limit) *Let* $\{I_n : M_{\lambda_n} \to \Omega_n\}$ *be a sequence of smooth embedded paper Moebius bands with* $\lambda_n \to \sqrt{3}$. *Then, up to isometry,* I_n *converges uniformly to the map giving the triangular Moebius band.*

1.3 Outline of the Proofs

Let $I : M_\lambda \to \Omega$ be a smooth embedded paper Moebius band. A *bend* on Ω is a line segment B' which cuts across Ω and has its endpoints in the boundary. It is a classic fact that Ω has a continuous foliation by bends. See §2.1. The bend foliation may not be unique, but we choose a bend foliation once and for all. The bends in the foliation vary continuously and are pairwise disjoint.

Given a bend B', we call the inverse image $B = I^{-1}(B')$ a *pre-bend*. It is a classic fact that pre-bends are line segments. (Proof: If not, then there are points $p, q \in B$ whose distance in M_λ is less than the distance in $\boldsymbol{R}^3$ between $I(p)$ and $I(q)$. This contradicts the fact that $I : M_\lambda \to \boldsymbol{R}^3$ is distance non-increasing.) The inverse image of our bend foliation is a foliation of M_λ into pre-bends. This is just like the pinstriping in Figures 1a and 1b except that in the smooth case even the endpoints are disjoint.

We say that a *T-pattern* on Ω is a pair of bends which lie in perpendicular intersecting lines. Look again at the right sides of Figures 1a and 1b. We call the T-pattern *embedded* if the two bends are disjoint. In §2.2 we prove

Lemma 1.3 (T) *A smooth embedded paper Moebius band has an embedded T-pattern.*

Here is the idea. The space of pairs of unequal bends in our bend foliation has a 2-point compactification which makes it into the 2-sphere, S^2. We define a pair of odd functions on S^2 which detect a T-pattern when they have a common zero. We apply the Borsuk-Ulam Theorem to get a common zero. In §2.3 we prove

Lemma 1.4 (G) *A smooth embedded paper Moebius band with an embedded T-pattern has aspect ratio greater than* $\sqrt{3}$.

Here is the idea. Let (T', B') be the embedded T-pattern. We cut open M_λ along the pre-bend $T = I^{-1}(T')$, and the result is a bilaterally symmetric trapezoid τ. See Figure 2 below. We then solve an optimization problem which involves mapping τ into $\boldsymbol{R}^3$ with constraints coming from the geometry of trapezoids and T-patterns. The Main Theorem is an immediate consequence of Lemma T and Lemma G.

In §2.4 we prove the Triangular Limit Theorem by examining what the proof of Lemma G says about a minimizing sequence of examples.

1.4 Additional Material and Context

The proofs are done after §2, but I include some more material. In §3 I comment on the proofs and also give additional context. In §4 I give an elementary and self-contained proof of a special case of [**HN**, §3, Lemma 2], the result that underlies the existence of the bend foliation.

The topic of paper Moebius bands is adjacent to a number of different subjects. The paper [**CKS**] and [**DDS**] consider the related question of tying a piece of rope into a knot using as little rope as possible. The papers [**D**] and [**DL**] consider folded ribbon knots. [**DL**, Corollary 25] is in some sense a special case of our two results, and [**DL**, Conjecture 26] is a variant of the Halpern-Weaver Conjecture in the category of folded ribbon knots. Our Main Theorem incidentally resolves this folded ribbon knot conjecture. Some authors have considered "optimal Moebius bands" from other perspectives, either algebraic [**Sz**] or physical [**MK**], [**SH**]. I will discuss some of these things in §3.4.

In §3.5 I discuss multi-twist Moebius bands, and some new results about them, namely [**BS**], [**H**], and [**S3**].

This paper is an outgrowth of my earlier paper [**S1**]. In [**S1**] I (correctly) prove that $\lambda \geq \phi = (1+\sqrt{5})/2$, but I also make an idiotic mistake: Somehow I thought that when you cut open M_λ along a pre-bend you get a parallelogram. This mistake invalidates my final bound, a weird and forgettable algebraic number in $(\phi, \sqrt{3})$. This paper supersedes [**S1**] and is independent from it.

1.5 Acknowledgements

I thank Brienne Brown, Matei Coiculescu, Robert Connelly, Dan Cristofaro-Gardiner, Elizabeth Denne, Ben Halpern, Dmitry Fuchs, Javier Gomez-Serrano, Aidan Hennessey, Anton Izosimov, Jeremy Kahn, Rick Kenyon, Stephen D. Miller, Noah Montgomery, Sergei Tabachnikov, and Charles Weaver for helpful discussions about this subject. I especially thank Matei for suggesting that I try for a "mapping proof" of Lemma T as opposed to the kind of proof I had previously. That suggestion led me to find a really nice proof of Lemma T that greatly simplified this paper. Jeremy Kahn's remarks about the Borsuk-Ulam Theorem also helped streamline the proof of Lemma T. Finally, I thank the anonymous referees for insightful and helpful comments which improved the exposition of the paper.

2 Proofs of the Results

2.1 Existence of a Bend Foliation

Let $I : M_\lambda \to \Omega$ be a smooth embedded paper Moebius band. Recall that a *bend* is a line segment that cuts across Ω and has its endpoints in $\partial\Omega$.

Theorem 2.1 *Ω has a foliation by bends.*

We derive Theorem 2.1 from a classic result. As always for manifolds with boundary, the smoothness of the map I means that I has a smooth extension to a neighborhood of each boundary point. Thus, it makes sense to speak of the mean curvature of Ω even at points of $\partial\Omega$. Let Ω^o denote the interior of Ω. Let $U \subset \Omega^o$ denote the subset having nonzero mean curvature.

Lemma 2.2 *Each $p \in U$ lies in a unique bend γ. Every point along γ has nonzero mean curvature, even the endpoints.*

Lemma 2.2 follows from either of the two essentially identical results, [**CL**, p. 314, Lemma 2] and [**HN**, §3, Lemma 2]. In §4 I give an elementary and self-contained proof of Lemma 2.2.

Proof of Theorem 2.1: Let U^* denote the union of all the bends through points of U. We obtain U^* from U by adding in the endpoints of the bends. No two bends of U^* can intersect, even at the boundary. The reason: If they did intersect, then the point of intersection would have two distinct straight lines through it and hence zero mean curvature. This contradicts Lemma 2.2. Hence U^* actually has a foliation by bends. The fact that no two bends in this foliation intersect implies that they vary continuously.

Let τ' be a component of $\Omega - U^*$. If τ' has empty interior then τ' is a line segment, the limit of a sequence of bends. In this case τ' is also a bend. Suppose τ' has non-empty interior. Since all points of τ' have zero mean curvature, τ' lies in a single plane. (One way to see this is to note that the Gauss map is constant in τ'.) Let $\tau = I^{-1}(\tau')$. The map $I|_\tau : \tau \to \tau'$ is an isometric embedding between planar regions, and also the domain τ is convex – just a trapezoid. This implies that $I|_\tau$ is a global isometry and in particular maps line segments to line segments. Now we foliate τ by line segments interpolating between the two pre-bends in $\partial\tau$. The image under $I|_\tau$ of this foliation of τ is a bend foliation of τ'. Doing this construction on all such components, we get our bend foliation of Ω. ♠

2.2 Proof of Lemma T

Let $I : M_\lambda \to \Omega$ be a smooth embedded paper Moebius band. We first give some definitions.

Recall from §1.3 that a *pre-bend* is the pre-image of a bend. The pre-bends are embedded line segments in M_λ which have their endpoints in ∂M_λ.

The *centerline* of M_λ is the circle $([0,\lambda] \times \{1/2\})/\sim$. The *centerline of* Ω is the image of the centerline of M_λ under the map I. These centerlines are topological circles and I is a diffeomorphism between them.

Each bend u has exactly 2 unit vectors $\pm\overrightarrow{u}$ parallel to it. We call either one an *orientation* of u.

Intersection with the Centerline: We are in a Moebius band, so a pre-bend u, being embedded, must intersect the centerline exactly once. Here is an alternate proof: Let $\ell(\cdot)$ denote length. If $\ell(u) < \sqrt{1+\lambda^2}$ we can move u by an isometry so that it misses the vertical sides of $[0,\lambda] \times [0,1]$. But then u clearly intersects the centerline exactly once. So, if u intersects the centerline more than once, we have $\ell(u) \geq \sqrt{1+\lambda^2} > \lambda$. But $\partial\Omega = I(\partial M_\lambda)$ is a loop that contains the endpoints of the bend $I(u)$, and $\ell(I(u)) = \ell(u) > \lambda$. Hence $\ell(\partial\Omega) > 2\lambda$. But $\ell(\partial\Omega) = \ell(\partial M_\lambda) = 2\lambda$, a contradiction.

The Circle of Bends: The bend foliation of Ω guaranteed by Theorem 2.1 may not be unique. We simply choose one. Call it β. We mention again that the bends in β are segments which vary continuously and are pairwise disjoint. We parametrize the bends of β by $\boldsymbol{R}/2\pi$, as follows: Since I is an embedding, our result about pre-bends implies that each bend of Ω intersects the centerline of Ω exactly once. We associate to each bend the point where it intersects the centerline, and then we identify the centerline with $\boldsymbol{R}/2\pi$.

The Cylinder and the Sphere: Let Υ be the topological cylinder of pairs $(x_0, x_1) \in (\boldsymbol{R}/2\pi)^2$ with $x_0 \neq x_1$. A point $(x_0, x_1) \in \Upsilon$ corresponds to a pair (u_0, u_1) of unequal bends. We let $\overline{\Upsilon}$ be the compactification of Υ obtained by adding 2 points: ∂_+ (respectively ∂_-) is the limit of pairs (x_0, x_1) where x_1 is just ahead (respectively just behind) x_0 in the cyclic order on $\boldsymbol{R}/2\pi$. The space $\overline{\Upsilon}$ is homeomorphic to S^2, the 2-sphere. See §3.1 for an explicit homeomorphism. The map $\Sigma(x_0, x_1) = (x_1, x_0)$ extends to a continuous involution of S^2 that swaps the two points ∂_+ and ∂_-. The explicit homeomorphism in §3.1 conjugates Σ to the antipodal map of S^2.

Propagating the Orientations: We orient $\boldsymbol{R}/2\pi$. Let $(x_0, x_1) \in \Upsilon$. There is a unique embedded, locally linear, positively oriented path $t \to x_t$ in $\boldsymbol{R}/2\pi$ which joins x_0 and x_1. This path is short (respectively long) when (x_0, x_1) is near ∂_+ (respectively ∂_-). Let u_t be the bend associated to x_t. We write $\overrightarrow{u}_0 \rightsquigarrow \overrightarrow{u}_1$ when there is a continuous orientation of the bends $\{u_t\}$ that restricts to $\overrightarrow{u}_0$ and $\overrightarrow{u}_1$. Note that $-\overrightarrow{u}_0 \rightsquigarrow -\overrightarrow{u}_1$ and, since Ω is a Moebius band, $\overrightarrow{u}_1 \rightsquigarrow -\overrightarrow{u}_0$. Also $\overrightarrow{u}_1 \to \pm\overrightarrow{u}_0$ when $(x_0, x_1) \to \partial_\pm$.

The Map: Let m_j be the midpoint of u_j. Using the dot product $(\cdot)$ and the cross product $(\times)$ define $F = (g, h) : \Upsilon \to \boldsymbol{R}^2$, where

$$g(x_0, x_1) = \overrightarrow{u}_0 \cdot \overrightarrow{u}_1, \qquad h(x_0, x_1) = (m_0 - m_1) \cdot (\overrightarrow{u}_0 \times \overrightarrow{u}_1). \tag{2}$$

This definition is independent of the chosen orientation since $-\overrightarrow{u}_0 \rightsquigarrow -\overrightarrow{u}_1$. Also, F extends continuously S^2 with $F(\partial_\pm) = (\pm 1, 0)$. Since $\overrightarrow{u}_1 \rightsquigarrow -\overrightarrow{u}_0$ we have $F \circ \Sigma = -F$. Why? Well, clearly $g(x_1, x_0) = -g(x_0, x_1)$, and

$$h(x_1, x_0) = (m_1 - m_0) \cdot (\overrightarrow{u}_1 \times (-\overrightarrow{u}_0)) = (m_1 - m_0) \cdot (\overrightarrow{u}_0 \times \overrightarrow{u}_1) = -h(x_0, x_1).$$

The Borsuk-Ulam Theorem says that $(0, 0) \in F(S^2)$. Since $F(\partial_\pm) \neq (0, 0)$ we have $(0, 0) \in F(\Upsilon)$. See the remark below for a self-contained proof.

Endgame: Let (u_0, u_1) be the bends corresponding to $(x_0, x_1) \in F^{-1}(0, 0)$. First, u_0 and u_1 are disjoint because they belong to the same foliation. Second, $\overrightarrow{u}_0$ and $\overrightarrow{u}_1$ are orthogonal because $g(x_0, x_1) = 0$. Third, $\overrightarrow{u}_0$ and $\overrightarrow{u}_1$ and $m_0 - m_1$ are all orthogonal to $\overrightarrow{u}_0 \times \overrightarrow{u}_1$ because $h(x_0, x_1) = 0$, and this easily implies that u_0, u_1 are coplanar. Hence (u_0, u_1) is an embedded T-pattern. This proves Lemma T.

Remark: Here is a self-contained proof that $(0, 0) \in F(\Upsilon)$. Suppose not. If γ is a continuous path in S^2 which goes from ∂_+ to ∂_-, then $F(\gamma)$ goes from $(1, 0)$ to $(-1, 0)$, misses $(0, 0)$, and winds some half integer $w(\gamma)$ times around the origin. All choices of γ are homotopic to each other relative to $\partial_\pm$, so $w(\gamma)$ is independent of γ. But consider $\gamma' = \Sigma(\gamma)$, re-oriented so that it goes from ∂_+ to ∂_-. Since $F \circ \Sigma = -F$ the image $F(\gamma')$ is obtained by rotating $F(\gamma)$ by 180 degrees about $(0, 0)$ then re-orienting it so that it goes from $(1, 0)$ to $(-1, 0)$. But then $w(\gamma') = -w(\gamma)$, a contradiction.

2.3 Proof of Lemma G

Let ℓ denote arc length. Let $\bigtriangledown$ be a triangle with horizontal base. Let $\vee$ be the union of the two non-horizontal sides of $\bigtriangledown$.

Lemma 2.3 *If $\bigtriangledown$ has base $\sqrt{1+t^2}$ and height $h \geq 1$ then $\ell(\vee) \geq \sqrt{5+t^2}$, with equality iff $\bigtriangledown$ is isosceles and $h = 1$.*

Proof: This is an exercise in high school geometry. Let p_1, p_2, q be the vertices of $\bigtriangledown$, with p_1, p_2 lying on the base. Let p_2' be the reflection of p_2 in the horizontal line through q. Note that $\bigtriangledown$ is isosceles iff p_1, q, p_2' are collinear. By symmetry, the triangle inequality, and the Pythagorean Theorem,

$$\ell(\vee) = \|p_1 - q\| + \|q - p_2'\| \geq \|p_1 - p_2'\| = \sqrt{1 + t^2 + 4h^2} \geq \sqrt{5 + t^2}.$$

We get equality if and only if p_1, q, p_2' are collinear and $h = 1$. ♠

Let $I : M_\lambda \to \Omega$ be a smooth embedded paper Moebius band with an embedded T-pattern. Let $S' = I(S)$ for any $S \subset M_\lambda$. We have $\ell(\gamma) = \ell(\gamma')$ for any curve $\gamma \subset M_\lambda$.

We rotate Ω so that one of the bends of the T-pattern, T', lies in X-axis and the other bend, B', lies in the negative ray of the Y-axis. Next, we let $B = I^{-1}(B')$ and $T = I^{-1}(T')$ be the corresponding pre-bends. We emphasize that B and T are disjoint embedded line segments.

We cut M_λ open along T to get a bilaterally symmetric trapezoid τ. We normalize τ so that the parallel sides are horizontal. Reflecting τ in the coordinate axes if needed, we arrange that u, v, w, x are mapped to Ω as in Figure 2. The quantities t and b (which are both positive in the case depicted) respectively denote the horizontal displacements of T and B.

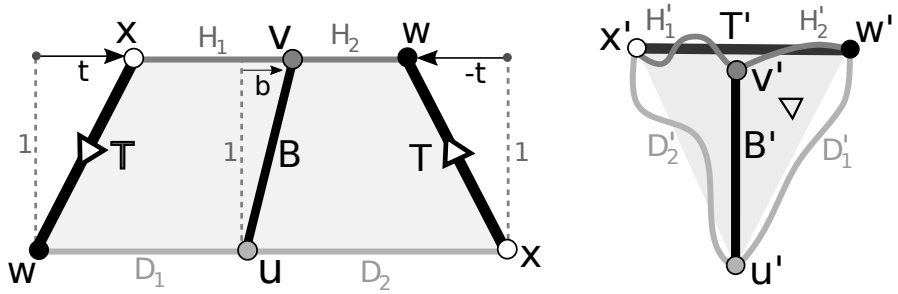

Figure 2: The trapezoid τ (left) and the T-pattern (right).

With Lemma 2.3 in mind, note that the shaded triangle $\bigtriangledown$ has

$$\text{base} = \ell(T') = \ell(T) = \sqrt{1+t^2}, \qquad \text{height} > \ell(B') = \ell(B) = \sqrt{1+b^2} \geq 1.$$

Let $H = H_1 \cup H_2$ and $D = D_1 \cup D_2$. We have $H', D' \subset \boldsymbol{R}^3$, so you should imagine you are floating in space above Figure 2 and looking down. Now H' connects the endpoints of T'. Also, D' connects the endpoints of T' and contains u. From this structure, and from Figure 2 (left), we have

$$\begin{aligned} \ell(H) + \ell(D) &= 2\lambda. \\ \ell(D) - 2t &= \ell(H). \\ \sqrt{1+t^2} = \ell(T') &\leq \ell(H') = \ell(H). \\ \sqrt{5+t^2} <^* \ell(\vee) &\leq \ell(D') = \ell(D). \end{aligned} \tag{3}$$

The starred inequality is Lemma 2.3. Equation 3 give us

$$\begin{aligned} \alpha(t) &:= \sqrt{1+t^2} + \sqrt{5+t^2} < \ell(H) + \ell(D) = 2\lambda. \\ \beta(t) &:= 2\sqrt{5+t^2} - 2t < 2\ell(D) - 2t = \ell(D) + \ell(H) = 2\lambda. \end{aligned} \tag{4}$$

Hence

$$2\lambda > \max(\alpha(t), \beta(t)). \tag{5}$$

Let $t_0 = 1/\sqrt{3}$. We have

- $\alpha(t_0) = \beta(t_0) = 2\sqrt{3}$.
- α is increasing on $(0, \infty)$. Hence $\alpha(t) > 2\sqrt{3}$ if $t > t_0$.
- β is decreasing on $\boldsymbol{R}$. Hence $\beta(t) > 2\sqrt{3}$ if $t < t_0$.

Hence $\lambda > \sqrt{3}$. This proves Lemma G.

Our proof of the Main Theorem is done.

2.4 Proof of the Triangular Limit Theorem

Figure 3 shows what Figure 2 looks like when we make the construction for the triangular Moebius band with respect to the T-pattern depicted on the right side of Figure 1b.

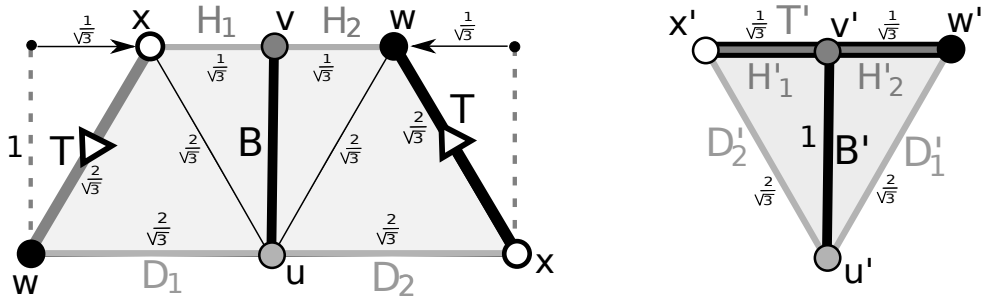

Figure 3: Figure 2 for the triangular Moebius band.

Let $\{I_n : M_{\lambda_n} \to \Omega_n\}$ be as in the Triangular Limit Theorem. We run the construction of Lemma G for each n and analyze what happens as $n \to \infty$. We use the same notation as in the proof of Lemma G, except that we add subscripts to indicate the dependence on n.

The Range: Since $\max(\alpha(t_n), \beta(t_n)) \to 2\sqrt{3}$ we have $t_n \to 1/\sqrt{3}$. Hence $\ell(T'_n) \to 2/\sqrt{3}$. Since $\lambda_n \to \sqrt{3}$ and $\ell(\bigtriangledown_n) \leq 2\lambda_n$, we have

$$\limsup \ell(\bigtriangledown_n) \leq 2\sqrt{3}. \tag{6}$$

The base of $\bigtriangledown_n$ converges to $2/\sqrt{3}$ and the height is always greater than 1. Lemma 2.3 combines with Equation 6 to show that $\bigtriangledown_n$ converges (up to isometries) to an isosceles triangle of base $2/\sqrt{3}$ and height 1. This is the shaded equilateral triangle $\bigtriangledown$ shown in Figure 3 (right). We normalize by isometries so that we get actual convergence.

The Domain: Since $\ell(\partial\Omega_n) - \ell(\bigtriangledown_n) \to 0$ and also v'_n converges to the midpoint of T'_n, all the slack goes out of Equation 3, and

$$\lim \ell(H'_{n,1}) = \lim \ell(H'_{n,2}) = 1/\sqrt{3}, \quad \lim \ell(D'_{n,1}) = \lim \ell(D'_{n,2}) = 2/\sqrt{3}. \tag{7}$$

Since $\ell(H_{n,1}) = \ell(H'_{n,1})$, etc. τ_n converges (up to isometries) to τ, the trapezoid in Figure 3 (left). We normalize so that we get actual convergence.

The Boundary Map: The arcs $H'_{n,1}, H'_{n,2}, D'_{n,1}, D'_{n,2}$ converge as sets to the line segments connecting their endpoints because $\ell(\partial\Omega_n) - \ell(\bigtriangledown_n) \to 0$. Since I_n is length preserving, I_n converges uniformly to a linear isometry when restricted to each of $H_{n,1}, H_{n,2}, D_{n,1}, D_{n,2}$. Hence I_n converges on ∂M_{λ_n} to the piecewise linear isometry associated to the triangular Moebius band.

The Whole Map: We divide M_λ into 3 triangles. See Figure 4.

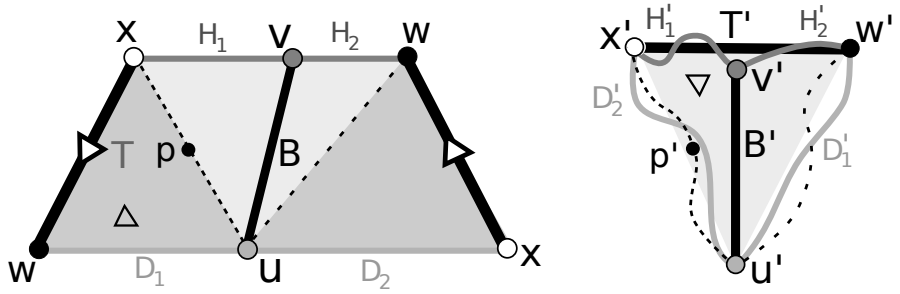

Figure 4: Figure 2 revisited

Consider the restriction of I_n to the left triangle $\triangle_n$. First, I_n is a linear isometry on $\overline{w_n x_n} = T_n$. Second, I_n converges to a linear isometry on $\overline{w_n u_n} = D_{n,1}$. Third, I_n converges to a linear isometry on $\overline{x_n u_n}$ because $\|x'_n - u'_n\| \to \|x_n - u_n\|$ and I_n is distance non-increasing. In summary, I_n converges to a linear isometry on $\partial\triangle_n$. Since I_n is distance non-increasing, this implies that I_n converges to a linear isometry on $\triangle_n$. The same argument works for the other 2 triangles. Hence I_n converges to the piecewise linear isometry associated to the triangular Moebius band.

Our proof of the Triangular Limit Theorem is done.

Remark: The proof is done, but we have a bit more to say. Let p_n be the midpoint of $\overline{x_n u_n}$. The point p'_n converges to the midpoint of $\overline{x'_n u'_n}$. The bend β'_n through p'_n has its endpoints on $H'_{n,1}$ and $D'_{n,1}$, and this forces one endpoint of β'_n to converge to x'_n and the other to u'_n. This means the pre-bend $\beta_n = I_n^{-1}(\beta'_n)$ converges to $\overline{x_n u_n}$. In other words, the left dotted line in Figure 4 is, for large n, quite close to a pre-bend. The same argument works for the right dotted line. From this, we see that the pre-bend foliation of M_{λ_n} converges to the pinstriping shown in Figures 1a (left) and 1b (left). Likewise, the bend foliation of Ω_n converges to the pinstriping shown in Figures 1a (right) and 1b (right).

3 Discussion

3.1 An Explicit Homeomorphism

Referring to the proof of Lemma T, here we give an explicit homeomorphism from S^2 to $\overline{\Upsilon}$. We identify ∂_+ and ∂_- respectively with the north and south pole of S_2. We parametrize $S^2 - \partial_\pm$ by (θ, ϕ), where $\theta \in \boldsymbol{R}/2\pi$ is the longitude and $\phi \in (0, \pi)$, the angle with ∂_+, is the latitude. The antipodal map is $(\theta, \phi) \to (\pi + \theta, \pi - \phi)$. We get a homeomorphism between $S^2 - \partial_\pm$ and Υ with the correspondence $(\theta, \phi) \leftrightarrow (X_{\theta-\phi}, X_{\theta+\phi})$. This conjugates Σ to the antipodal map, and extends to a homeomorphism between S^2 and $\overline{\Upsilon}$.

3.2 Paths of Oriented Lines

Anton Izosimov and Sergei Tabachnikov independently suggested to me the following generalization of Lemma T.

Lemma 3.1 *Suppose $\{L_t |\ t \in [0,1]\}$ is a continuous family of oriented lines in $\boldsymbol{R}^3$ such that $L_1 = L_0^{\rm opp}$, the same line as L_0 but with the opposite orientation. Then there exist parameters $r, s \in [0,1]$ such that L_r and L_s are perpendicular intersecting lines.*

Proof: This has the same proof as Lemma T, once we observe that our function h, defined in Equation 2, is more natural than we have let on. The points m_0, m_1 in the definition of h could be any points on u_0, u_1 and we would get the same result. g and h are invariants of pairs of oriented lines. ♠

Sergei also suggested to me a beautiful alternate formalism for Lemma T: the *dual numbers*. These have the form $x + \epsilon y$ where $x, y \in \boldsymbol{R}$ and $\epsilon^2 = 0$. Relatedly, the *dual vectors* have the form $\overrightarrow{a} + \epsilon \overrightarrow{b}$, where $\overrightarrow{a}, \overrightarrow{b} \in \boldsymbol{R}^3$ and again $\epsilon^2 = 0$. In this context, the dot product of two dual vectors makes sense as a dual number. See [**HH**] for an exposition.

Each oriented line $\ell \subset \boldsymbol{R}^3$ gives rise to a dual vector $\xi_\ell = \overrightarrow{a} + \epsilon \overrightarrow{b}$ where $\overrightarrow{a}$ is the unit vector pointing in the direction of ℓ and $\overrightarrow{b} = \ell' \times \overrightarrow{a}$. Here $\ell' \in \ell$ is any point. All choices of ℓ' give rise to the same $\overrightarrow{b}$; this vector is called the *moment vector* of ℓ. This formalism identifies the space of oriented lines in $\boldsymbol{R}^3$ with the so-called *study sphere* consisting of dual vectors ξ such that $\xi \cdot \xi = 1$. The dual dot product $\xi_\ell \cdot \xi_m$ vanishes if and only if ℓ and m are perpendicular and intersect.

3.3 Interpretations of Smoothness at the Boundary

Our map $I : M_\lambda \to \Omega$ is a smooth isometric embedding. The domain of I is a smooth manifold with boundary. Whenever we have a situation like this, the notion *smoothness* at the boundary really means that we can extend the definition of I at each boundary point to a larger open manifold so that the extension is smooth. In our situation we can use compactness to say that there is some $\epsilon > 0$ such that I extends smoothly to

$$M_\lambda^\epsilon = [0, \lambda] \times (-\epsilon, 1 + \epsilon)/\sim, \qquad (0, y) \sim (\lambda, 1 - y). \tag{8}$$

A stronger interpretation would be that for some ϵ the extension is also an isometric embedding. With this interpretation the proof of Lemma 2.2 (given below in §4) would be easier. We wouldn't need to treat boundary points in a special way. A weaker interpretation would be that I is merely continuous on M_λ and a smooth isometric embedding on the interior of M_λ. Our standard interpretation steers a middle ground between these extremes.

Let us say that the Main Theorem$^\flat$ is the Main Theorem for the strong version kind of smooth embedded paper Moebius bands. Let us say that the Main Theorem$^\sharp$ is the Main Theorem for the weak version kind of smooth embedded paper Moebius bands. We use similar notation for other concepts. Obviously, our theorems imply our theorems$^\flat$, and in turn our theorems$^\sharp$ would imply our theorems. Actually the reverse is also true.

Given a smooth$^\sharp$ embedded paper Moebius band we have a *trimming operation*: We can restrict I to the thinner Moebius band

$$[0, \lambda] \times (\epsilon, 1 - \epsilon)/\sim, \qquad (0, y) \sim (\lambda, 1 - y). \tag{9}$$

Then we can rescale and domain and range to get a smooth$^\flat$ embedded paper Moebius band of aspect ratio $\sqrt{3}/(1 - 2\epsilon)$. Applying the Main Theorem$^\flat$ we see that $\lambda > \sqrt{3}(1 - 2\epsilon)$. Letting $\epsilon \to 0$ we get $\lambda \geq \sqrt{3}$. Suppose $\lambda = \sqrt{3}$. Then we consider a sequence of trimmings with $\epsilon \to 0$. The Triangular Limit Theorem$^\flat$ says that these converge to the triangular Moebius band. But this implies that our map $I : M_\lambda \to \Omega$ is the triangular Moebius band. This is a contradiction. Hence $\lambda > \sqrt{3}$. Thus, the Main Theorem$^\flat$ and the Triangular Limit Theorem$^\flat$ imply the Main Theorem$^\sharp$. A similar argument shows that the Triangular Limit Theorem$^\flat$ implies the Triangular Limit Theorem$^\sharp$.

In short, we really don't need to fuss about the exactly what happens at the boundary of a smooth embedded paper Moebius band.

3.4 Related Topics

Square Peg: Around the time I got interested in the Halpern-Weaver Conjecture I had been thinking about the Toeplitz Square Peg Conjecture, which asks if every continuous loop in the plane contains 4 points which make the vertices of a square. See [**Mat**] for a fairly recent survey. One can view a T-pattern as a collection of 4 points in the boundary of the Moebius band which satisfy certain additional constraints – e.g. they are coplanar. Put this way, a T-pattern is sort of like a square inscribed in a Jordan loop.

Quadrisecants: The idea for Lemma T is also similar in spirit for the idea developed in [**DDS**] concerning 4 collinear points on a knotted loop. These so-called *quadrisecants* play a role similar to Lemma T in getting a lower bound for the length of a knotted rope.

Folded Ribbon Knots: Elizabeth Denne pointed out to me the connection between paper Moebius bands and *folded ribbon knots*. Her paper with Troy Larsen [**DL**] gives a formal definition of a folded ribbon knot and has a wealth of interesting constructions, results, and conjectures. See also [**D**], a survey article.

Informally, folded ribbon knots are the objects you get when you take a flat cylinder or Moebius band, fold it into a knot, and then press it into the plane. Associated to a folded ribbon knot is a polygon, which comes from the centerline of the object. Even though the ribbon knot lies entirely in the plane, one assigns additional combinatorial data which keeps track of "infinitesimal" under and over crossings as in a knot diagram. So the associated centerline is really a knot (or possibly the unknot).

[**DL**, Corollary 25] proves our Main Theorem in the category folded ribbon Moebius bands whose associated centerline is a triangle. This is a finite dimensional problem. [**DL**, Conjecture 26] says that [**DL**, Corollary 25] is true without the very strong triangle restriction. This is an infinite dimensional problem like the Halpern-Weaver Conjecture. The combination of our Main Theorem and the Triangular Limit Theorem implies [**DL**, Conjecture 26]. One takes arbitrarily nearby smooth approximations, as in [**HW**], and then applies our results to them.

3.5 More Twists

The Halpern-Weaver Conjecture is one of infinitely many similar kinds of questions one can ask about paper Moebius bands. For instance, one translate the many conjectures made in [**DL**] about folded ribbon knots into the broader language of paper geometry.

Twisted Cylinders: One can make a *twisted cylinder* by taking a $1 \times \lambda$ strip of paper, giving it an even and nonzero number of twists, and then joining the ends together. The essential feature of twisted cylinders is that their two boundary components make a nontrivial link.

There are two optimal limiting shapes which have interpretations as folded ribbon knots. Both are folding patterns which wrap a 1×2 strip 4 times around a right-angled isosceles triangle. In [**S3**] I prove that a twisted cylinder has aspect ratio greater than 2 and that any minimizing sequence converges on a subsequence to one of the two optimal models. This result also confirms the $n = 1$ case of [**DL**, Conjecture 39]. The proof is somewhat similar to what I do in this paper, though the fine-scale details are different. Noah Montgomery (private communication) independently came up with a proof of the cylinder result. His elegant proof is different than mine.

Three Twist Moebius Bands: What happens when you insist that a paper Moebius band have least 3 twists? An essential feature of these objects is that their boundaries are knotted. I think it follows from the Triangular Limit Theorem and from compactness that there is some ϵ_0 such that the aspect ratio of a multi-twisted paper Moebius band is at least $\sqrt{3} + \epsilon_0$.

Brienne Brown did some experiments with these objects and found two candidate optimal models. We call these the *crisscross* and the *cup*. Both are made from a 1×3 strip of paper. The crisscross is planar, and has an interpretation as a folded ribbon knot. The cup is not-planar: It is a double wrap of 3 mutually orthogonal right-angled isoceles triangles arranged like 3 faces of a tetrahedron. We wrote about this in [**BS**], and conjecture there that $\lambda > 3$ for an embedded multi-twisted paper Moebius band.

Multi-Twist Examples: Recently, Aidan Hennessey [**H**] proved the very surprising result that one can make a cylinder or a Moebius band with any number of twists using a 1×8 strip. For Moebius bands only, his bound is better: you can do it with a 1×6.25 strip of paper.

4 Appendix: Proof of Lemma 2.2

We give a self-contained proof of Lemma 2.2. Let S^2 be the unit 2-sphere. The *Gauss map*, which is well defined and smooth on any simply-connected subset of Ω, associates to each point $p \in \Omega$ a unit normal vector $n_p \in S^2$. Let dn_p be the differential of the Gauss map at p. Since the curvature Ω is 0 everywhere, dn_p has a nontrivial kernel. The point p has nonzero *mean curvature* if and only if dn_p has nontrivial image.

Let U be as in Lemma 2.2, the subset of Ω^o with nonzero mean curvature. Let $p \to n_p$ be a local choice of the Gauss map. We can rotate and translate so that near the origin U is the graph of a function

$$F(x, y) = Cy^2 + \text{higher order terms.} \tag{10}$$

Here $C > 0$ is some constant. The normal vector at the origin is $n_0 = (0, 0, 1)$. The vector $v_0 = (1, 0, 0)$ lies in the kernel of dn_0. Let $w_0 = (0, 1, 0)$. Let Π_0 be the plane spanned by w_0 and n_0. The image of $\Pi_0 \cap U$ under the Gauss map is (near n_0) a smooth regular curve tangent to w_0 at n_0. The sign depends on the choice of local Gauss map.

Working locally, we have three smooth vectorfields:

$$p \to n_p, \qquad p \to v_p, \qquad p \to w_p = v_p \times n_p. \tag{11}$$

Here v_p is the kernel of dn_p and $\times$ denote the cross product. Let Π_p be the plane through p and spanned by w_p and n_p. From our analysis of the special case, and from symmetry, the image of $\Pi_p \cap U$ under the Gauss map is (near n_p) a smooth regular curve tangent to w_p at n_p. The *asymptotic curves* are the smooth curves everywhere tangent to the v vector field.

Lemma 4.1 *The asymptotic curves are line segments.*

Proof: Let γ be an asymptotic curve. The Gauss map is constant along γ. Each point in γ has a small neighborhood V which is foliated by asymptotic curves that transversely intersect each plane Π_p when $p \in \gamma \cap V$. Hence the image of V under the Gauss map equals the image of $\Pi_p \cap V$ under the Gauss map. This latter image is a smooth regular curve tangent to w_p at n_p. Since this is true for all $p \in \gamma \cap V$ and since n_p is constant along γ, w_p is constant along γ. Hence v_p is constant along γ. Hence γ is a line segment. ♠

The nonzero mean curvature implies that γ is the unique line segment through any of its interior points. We first rule out the possibility that γ reaches ∂U before it reaches $\partial\Omega$. Assume for the sake of contradiction that this happens. We normalize as in Equation 10.

We now allow ourselves the liberty of dilating our surface. This dilation preserves all the properties we have discussed above. By focusing on a point of γ sufficiently close to ∂U and dilating, we arrange the following:

- A neighborhood $\mathcal{V}$ of Ω^o is the graph of a function over the disk of radius 3 centered at the origin.
- Given $p \in \mathcal{V}$ let p' be the projection of p to the XY-plane. We have $|p_1' - p_2'| > (2/3)|p_1 - p_2|$ for all $p_1, p_2 \in \mathcal{V}$.
- $\gamma \subset U$ contains the arc connecting $(0,0,0)$ to $(3,0,0)$, but $(0,0,0) \notin U$.

Let $a \in (0,3)$. At $(a,0,0)$ we have $v_a = (1,0,0)$ and $w_a = (0,1,0)$ and $n_a = (0,0,1)$. Let Π_a be the plane $\{X = a\}$. Near $(a,0,0)$, the intersection $U_a = U \cap \Pi_a$ is a smooth curve tangent to w_a at $(a,0,0)$.

Let $\zeta = (1,0,0)$. Fix $\delta > 0$. By continuity and compactness, the asymptotic curves through points of U_1 sufficiently near ζ contain line segments connecting points on U_2 to points on U_δ. Call these *connectors*. There exists a canonical map $\Phi_\delta : U_1 \to U_\delta$ defined in a neighborhood of ζ: The points $q \in U_1$ and $\Phi_\delta(q) \in U_\delta$ lie in the same connector.

Lemma 4.2 *Φ_δ expands distances by less than a factor of 3.*

Proof: Let ℓ_1 and ℓ_2 be two connectors. Let $a_j = \ell_j \cap U_1$. Let $b_j = \ell_j \cap U_\delta$. For any set S let S' be the projection of S to $\boldsymbol{R}^2$. We have the bounds

$$\frac{|a_1' - a_2'|}{|a_1 - a_2|}, \frac{|b_1' - b_2'|}{|b_1 - b_2|} \in \left[\frac{2}{3}, 1\right], \qquad \frac{|a_j' - b_j'|}{\text{length}(\ell_j')} < 2.$$

Geometrically, a_j' is very nearly the midpoint of ℓ_j' and b_j' is the closer of the two endpoints. Since ℓ_1' and ℓ_2' are planar and disjoint, our last inequality (and essentially a similar-triangles argument) gives $|b_1' - b_2'|/|a_1' - a_2'| < 2$. Putting everything together, we have $|b_1 - b_2|/|a_1 - a_2| < 3$. ♠

Fix $\epsilon > 0$. The mean curvature along U_δ tends to 0 as $\delta \to 0$. If we choose δ sufficiently small then the Gauss map expands distances along U_δ in

a neighborhood of $(\delta, 0, 0)$ by a factor of less than ϵ. Combining Lemma 4.2 and the fact that $n_q = n_{\Phi_\delta(q)}$, we see that the Gauss map expands distances by at most a factor of 3ϵ along U_1 in a small neighborhood of ζ. Since ϵ is arbitrary, $w_1 \in \ker(dn_\zeta)$. But $v_1 \in \ker(dn_\zeta)$ by definition. Hence dn_ζ is the trivial map. The contradicts the fact that $\zeta \in U$.

Now we know that the interior of γ lies in U. Next, we show that the mean curvature cannot vanish at an endpoint of γ. As discussed in §3.3, there is some $\epsilon > 0$ so that I has a smooth extension to the fatter open Moebius band M_λ^ϵ described in Equation 8. If we knew that this smooth extension was also an isometric embedding, we could just use our previous argument exactly as is. (Compare the discussion in §3.3.) But, even if the extension is not an isometric map, we can still use the essentially the same argument. This time our open disk of radius 3 is divided into two sides, a lightly shaded *familiar side* consisting of projections of points of Ω and a darkly shaded *mystery side* consisting of projections of points of $I(M_\lambda^\epsilon) - I(M_\lambda)$. The common boundary of these regions is curve, transverse to the x-axis, which is a projection of $I(\partial M_\lambda)$. Figure 5 shows what we are taking about.

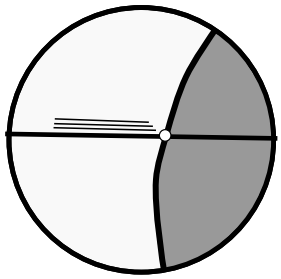

Figure 5: The connectors lie on the familiar side.

In the argument above, we can take the connectors to all lie in the familiar side, as shown in Figure 5. Then we can run exactly the same argument without ever entering into the mystery side. We then get the same contradiction as above. Hence the mean curvature does not vanish at an endpoint.

This completes the proof of Lemma 2.2.

5 References

[**BS**] B. E. Brown and R. E. Schwartz, *The crisscross and the cup: Two short 3-twist paper Moebius bands*, preprint 2023, arXiv:2310.10000

[**CF**] Y. Chen and E. Fried, *Mobius bands, unstretchable material sheets and developable surfaces*, Proceedings of the Royal Society A, (2016)

[**CK**] Carmen Chicone, N. J. Kalton, *Flat Embeddings of the Moebius Strip in* $\boldsymbol{R}^3$, Communications in Nonlinear Analysis 9 (2002), no. 2, pp 31-50

[**CKS**] J. Cantarella, R. Kusner, J. Sullivan, *On the minimum ropelength of knots and links*, Invent. Math. **150** (2) pp 257-286 (2003)

[**CL**], S.-S. Chern and R. K. Lashof, *On the total curvature of immersed manifolds*, Amer. J. Math. **79** (1957) pp 306–318

[**D**] E. Denne, *Folded Ribbon Knots in the Plane*, The Encyclopedia of Knot Theory (ed. Colin Adams, Erica Flapan, Allison Henrich, Louis H. Kauffman, Lewis D. Ludwig, Sam Nelson) Chapter 88, CRC Press (2021)

[**DL**] E. Denne, T. Larsen, *Linking number and folded ribbon unknots*, Journal of Knot Theory and Its Ramifications, Vol. 32 No. 1 (2023)

[**DDS**] E. Denne, Y. Diao, J. M. Sullivan, *Quaadrisecants give new lower bounds for the ropelength of a knot*, Geometry&Topology 19 (2006) pp 1–26

[**FT**], D. Fuchs, S. Tabachnikov, *Mathematical Omnibus: Thirty Lectures on Classic Mathematics*, AMS 2007

[**H**] A. Hennessey, *Constructing many-twist Möbius bands with small aspect ratios*. arXiv:2401:14639 (2024)

[**HF**], D.F. Hinz, E. Fried, *Translation of Michael Sadowsky's paper 'An elementary proof for the existence of a developable MÖBIUS band and the attribution of the geometric problem to a variational problem'*. J. Elast. 119, 3–6 (2015)

[**HH**], A. A. Harkin and J. B. Harkin, *Geometry of Generalized Complex Numbers*, Mathematics Magazine **77** (2), pp 118-129 (2004)

[**HL**], P. Hartman and L. Nirenberg, *On spherical maps whose Jacobians do not change sign*, Amer. J. Math. **81** (1959) pp 901–920

[**HW**], B. Halpern and C. Weaver, *Inverting a cylinder through isometric immersions and embeddings*, Trans. Am. Math. Soc **230**, pp 41–70 (1977)

[**KU**], Kurono, Yasuhiro and Umehara, Masaaki, *Flat Möbius strips of given isotopy type in $\boldsymbol{R}^3$ whose centerlines are geodesics or lines of curvature*, Geom. Dedicata 134 (2008), pp 109-130

[**MK**] L. Mahadevan and J. B. Keller, *The shape of a Möbius band*, Proceedings of the Royal Society A (1993)

[**Ma1**] B. Matschke, *A survey on the Square Peg Problem*, Notices of the A.M.S. **Vol 61.4**, April 2014, pp 346-351.

[**RR**] T. Randrup, P. Rogan, *Sides of the Möbius Strip*, Arch. Math. 66 (1996) pp 511-521

[**Sa**], M. Sadowski, *Ein elementarer Beweis für die Existenz eines abwickelbaren MÖBIUSschen Bandes und die Zurückführung des geometrischen Problems auf einVariationsproblem*. Sitzungsberichte der Preussischen Akad. der Wissenschaften, physikalisch-mathematische Klasse 22, 412–415.2 (1930)

[**Sab**] I. Kh. Sabitov, *Isometric immersions and embeddings of a flat Möbius strip into Euclidean spaces*, Izv. Math. **71** (2007), pp 1049-1078

[**S1**] R. E. Schwartz, *An improved bound on the optimal paper Moebius band*, Geometriae Dedicata, 2021

[**S2**] R. E. Schwartz, *The Optimal Paper Moebius Band: A Friendly Account*, preprint, 2023

[**S3**] R. E. Schwartz, *The Optimal Twisted Paper Cylinder*, preprint 2023, arXiv:2309.14033

[**SH**] E. L. Starostin, G. H. M. van der Heijden, *The shape of a Möbius Strip*, Nature Materials **6** (2007) pp 563 – 567

[**Sz**] G. Schwarz, *A pretender to the title "canonical Moebius strip"*, Pacific J. of Math., **143** (1) pp. 195-200, (1990)

[**T**] Todres, R. E., *Translation of W. Wunderlich's On a Developable Möbius band*, Journal of Elasticity **119** pp 23–34 (2015)

[**W**] W. Wunderlich, *Über ein abwickelbares Möbiusband*, Monatshefte für Mathematik **66** pp 276–289 (1962)